Electronic structure and spin-resolved photoemission of Cu_3Au (001)

1993 J. Phys.: Condens. Matter 5 4711

(http://iopscience.iop.org/0953-8984/5/27/015)

J. Phys.: Condens. Matter 5 (1993) 4711–4720. Printed in the UK

Electronic structure and spin-resolved photoemission of Cu_3Au (001)

S V Halilov, H Gollisch, E Tamura† and R Feder
Theoretische Festkörperphysik, Universität Duisburg, D-W-4100 Duisburg, Federal Republic of Germany

Received 10 March 1993, in final form 29 April 1993

Abstract. A fully relativistic Green function formalism is applied to calculate the layer-, $k_\parallel$- and double group symmetry-resolved densities of states (DOS) and the spin-resolved normal photoemission intensities produced by normally incident circularly polarized light for the (001) surface of Cu_3Au in its ordered phase. In the calculated photoemission spectra, a number of features can be ascribed to interband transitions in our simultaneously calculated bulk band structure, with a real self-energy correction of −0.45 eV for the lower and of 2.5 eV for the upper states. In addition, we identify seven features as due to surface states or surface resonances. A comparison with spin-resolved experimental data shows reasonable agreement with regard to existence, energy and preferential spin polarization (i.e. symmetry type of initial states) for most features.

1. Introduction

Both for its own sake and as a prerequisite for understanding an order–disorder phase transition, the electronic structure of the noble-metal alloy Cu_3Au has been studied very extensively by first-principles calculations (Lu *et al* 1992, Kudrnovsky *et al* 1991, Ginatempo *et al* 1990, Sohal *et al* 1990, Davenport *et al* 1988, and references therein) and by photoemission experiments (Löbus *et al* 1992, Schneider *et al* 1990, Sohal *et al* 1990, and references therein). The theoretical investigations—mostly in the framework of relativistic density functional theory—concentrated on the (infinite) bulk material, producing the occupied part of the band structure and the associated total and directional ($k_\parallel$-resolved) bulk densities of states.

In the present work, we investigate, for the prototype case of the (001) direction, the semi-infinite Cu_3Au system, i.e. we consider simultaneously bulk and surface properties. The electronic structure is characterized by the layer-, double group symmetry- and $k_\parallel$-resolved density of states, which we calculate—starting from a self-consistent bulk LMTO potential—by means of a recently developed fully relativistic Green function formalism (Halilov *et al* 1993, Tamura and Feder 1989). To make direct contact with photoemission experiments, especially with the first spin-resolved spectra as produced by circularly polarized synchrotron radiation (Schneider *et al* 1990), we apply simultaneously a fully relativistic 'one-step model' photoemission theory of the layer-KKR-type, which is a generalized version (Halilov *et al* 1993, Tamura and Feder (1991a, b) of the formalism developed by Ackermann and Feder (1985) (see also ch. 4 of Feder 1985). In addition to confirming, with some modifications, already known bulk features, in particular the

† Present address: LLNL University of California, PO Box 808, L-268 Livermore CA94550, USA.

0953-8984/93/274711+10$07.50

decomposition of the electronic structure into a Au- and a Cu-dominated part, we find in particular a wealth of occupied surface states and resonances located in the topmost atomic layer.

In section 2, we briefly recall the theoretical formalism and describe our model assumptions specific for the ordered $Cu_3Au(001)$ system. Our calculated results for the bulk band structure, the layer-resolved density of states and spin-resolved photoemission are presented and discussed in section 3. In particular, we point out departures from earlier bulk results, discuss the new surface features and compare our calculated spin-resolved photoemission spectra with experiment.

2. Theory

A fully relativistic Green function formalism for semi-infinite crystalline systems, which yields layer-projected densities of states (Tamura and Feder 1989) and spin-resolved photoemission intensities (Tamura and Feder 1991a, b and references therein), has recently been extended to handle several atoms in the two-dimensional unit cell (Halilov *et al* 1993). We recall in particular that the Green function treatment of the initial state allows, in contrast to an earlier Bloch wave treatment, an *a priori* incorporation of the hole lifetime in photoemission and a convenient determination of electronic surface states. Simultaneously, the relativistic bulk band structure for occupied and unoccupied states can be obtained.

The geometry of bulk Cu_3Au can be viewed as a sequence of two alternating monoatomic layers along the (001) direction such that one layer has one Au and one Cu 'crystal-atom' in the two-dimensional unit cell and the other layer has two Cu crystal-atoms. For the $Cu_3Au(001)$ surface (figure 1), we assume a simple truncation of the bulk such that the topmost monoatomic layer has one Au and one Cu crystal-atom per cell and the second layer has two Cu crystal-atoms. The $k_\parallel$-resolved 'layer density of states' (LDOS) relates to such monolayers and is further decomposed with respect to the two types of atom and/or with respect to the relativistic double group symmetry types Δ_6 and Δ_7.

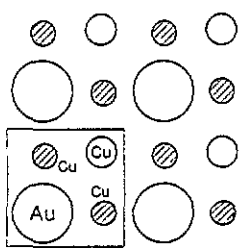

Figure 1. Schematic top view of the $Cu_3Au(001)$ surface: topmost layer with Au and Cu atoms (large and small empty circles) and second layer with Cu atoms only (small hatched circles). The square indicates the 2D unit cell.

The effective complex potential was constructed as follows. We first performed a self-consistent LMTO calculation, which is scalar-relativistic throughout and includes spin–orbit coupling in the last cycle, for bulk Cu_3Au with lattice constant 7.08 bohr using the von Barth–Hedin (1972) exchange correlation approximation. The atomic sphere radii in this LMTO calculation were chosen to ensure charge neutrality, yielding values of 3.073 bohr and 2.645 bohr for Au and Cu, respectively. The resulting real potential was then cast into the muffin-tin form. The radii of the touching Au and Cu spheres were chosen such as to minimize discontinuities, which gave a radius of 2.63 bohr and 2.33 bohr, respectively. We note that the occupied bulk energy bands obtained from this muffin-tin potential by

our layer-KKR method are practically the same as those from the original LMTO calculation. For photoemission purposes, the uniform part of this potential is replaced by a 'self-energy corrected' inner potential, which is energy-dependent and has an imaginary part to account for lifetime effects. As we have no first-principles knowledge of this inner potential we model it by parameters, the values of which have to be verified *ex post facto* by the agreement between calculated and measured photoemission spectra. We thus arrive at a real part V_r of the inner potential of 15.5 eV (below the vacuum level) for the occupied states and of 13 eV for unoccupied states at energies between about 10 and 20 eV above the vacuum level. Strictly speaking, V_r should of course decrease continuously with energy, but such refinement seems unwarranted at the present stage. The imaginary part is taken as $V_{i1} = (E-E_F)\times 0.025\,\text{eV}$ for occupied states of energy E, i.e. linearly increasing away from the Fermi energy E_F, and for the unoccupied states as $V_{i2} = -0.5\,\text{eV}/-1.0\,\text{eV}$ for photon energy $h\nu = 12\,\text{eV}/24\,\text{eV}$. For the surface potential barrier, we take a step model, which is reflecting for the occupied states and non-reflecting (but refracting) for the unoccupied states. Its location d_b above the topmost internuclear plane has been determined as $0.18a$ (where a is the bulk lattice constant) by detailed comparison with surface state energies as measured with high precision by Courths and co-workers (Courths 1992). Test calculations using the two-parameter JJJ model for the surface barrier (Jones *et al* 1984, Jennings *et al* 1988) produced small changes in the intensities but did not change the binding energies of the occupied surface states, which we are interested in here. For a study of the (unoccupied) image potential states, a surface barrier with image asymptotics (like the JJJ model) would of course be mandatory.

3. Results and discussion

In the following, we present bulk band structure and layer density of states results firstly for their own sake and secondly in view of interpreting a typical pair of calculated spin-resolved photoemission spectra (which will later be shown to agree reasonably well with experiment).

Consistent with the photoemission spectra, the occupied bulk bands (see figure 2) have also been calculated using the real inner potential part $V_r = 15.50\,\text{eV}$. They are identical with our original LMTO bands except for a downward shift of 0.45 eV (with respect to the Fermi level), since our LMTO V_r is 15.05 eV. This shift certainly contains the real part of the quasi-particle self-energy correction. Part of it may however also be due to shortcomings of the local-density approximation to exchange and correlation, which may lead to noticeable shifts of the Fermi level when, as is the case for the noble metals, E_F lies in a region of very small density of states. These findings are already known from the pure noble metals: band structure calculations (Jepsen *et al* 1981, MacDonald *et al* 1982), which employed very similar methods as the present work, produced initial-state energy eigenvalues, which are displaced upward in energy by about 1 eV for Ag and by about 0.4 eV for Cu and Au relative to experimental values obtained by photoemission (Courths *et al* 1984, and references therein). Note that the displacement for Cu and Au is actually about the same as the one required in the present case of Cu_3Au. For the pure noble metals, a closer alignment of calculated and experimental initial state bands has been reached by employing a potential with Xα exchange and by appropriately fitting the parameter α (Eckardt *et al* 1984 and Tamura *et al* 1989) individually for each metal. This procedure is, however, of the same *ad hoc* nature as our fitting of a real-part correction to the inner potential. Both are only a second best to a many-body treatment of the initial-state self-energy and to taking account of the non-locality of exchange and correlation.

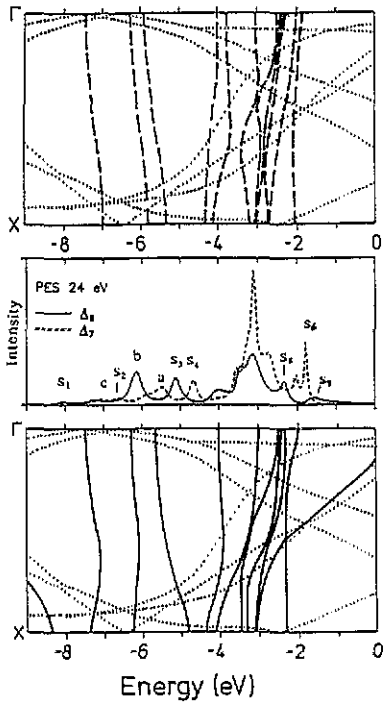

Figure 2. Bulk band structure of Cu_3Au along $\Gamma(\Delta)$ X: occupied states of symmetry types Δ_7 (broken curves in top panel) and Δ_6 (full curves in bottom panel) together with empty-state bands of symmetry-type Δ_6 shifted downward by photon of energy 24 eV (dotted curves). The middle panel shows spin-resolved normal photoemission spectra calculated for normally incident circularly polarized photons of energy 24 eV with surface barrier location $d_b = 0.18a$: from Δ_6 initial states (full curve) and Δ_7 initial states (broken curve).

For the occupied bulk states, our band structure (see figure 2)—if shifted again upward by the just-discussed self-energy correction of 0.45 eV—essentially agrees with earlier calculations by Davenport *et al* (1988), Ginatempo et al (1990) and Sohal *et al* (1990). We can therefore refer to its detailed discussion given in these papers. There are however some quantitative differences. Our Cu-like bands are about 0.15 eV lower in energy, which is slightly closer to experiment, but still too high by 0.3–0.45 eV (compare also the *ad hoc* downward shift needed in these papers, and Courths 1992). For the Au-dominated set of bands below 4.5 eV, our lowest-energy value at the Γ point is about 0.15 eV higher than in figure 5 of Davenport *et al* (1988) and in figure 2(*a*) of Sohal *et al* (1990), and its separation from the next-higher eigenvalue at Γ is 1.21 eV as compared to 1.14 and 1.18 eV in these two papers. Since this separation is caused by the spin–orbit interaction, we therefore obtain—following the detailed analysis of Davenport *et al* (1988)—a slightly larger spin–orbit parameter ξ. The origin of these discrepancies can unfortunately not be definitely identified on the grounds of the information available to us, but there are some clues. All calculations were performed relativistically and self-consistently in the framework of density functional formalism using a local density approximation (LDA). For the solution of the relativistic single-particle equations, Ginatempo *et al* (1990) and Sohal *et al* (1990) employed, like the present work, the LMTO method, but with equal atomic sphere radii for Au and Cu rather than different radii (3.073 and 2.645 bohr) as in our work. This is likely to give rise to some modification of the bands. Davenport *et al* (1988) used a linear augmented Slater-type orbital method with muffin-tin sphere radii close to the ones obtained by us after casting our self-consistent potential into the muffin-tin form. In contrast to our work, however, these radii were used throughout the self-consistency cycle. Their exchange correlation approximation (Hedin and Lundquist 1971) is fairly close to ours (von Barth and Hedin 1972).

The central panel of figure 2 shows calculated spin-resolved photoemission spectra

arising from initial states of double group symmetry types Δ_6 and Δ_7. In the one-step model framework of photoemission underlying our calculations, these states are of course half-space solutions of the Dirac equation. It is, however, interesting to find out which spectral features can be interpreted in the spirit of a three-step model in terms of direct transitions between bulk band states. To this end we also show, in the band structure panels, the upper-state bands of Δ_6, which can couple to the vacuum, shifted downward in energy by the photon energy 24 eV. A necessary (though, because matrix elements may vanish, not sufficient) condition for a bulk interband transition peak to occur is a crossing between a lower state band of the respective symmetry type with a shifted upper state band. We may thus interpret the peaks a, b and c in the Au region and most peaks in the Cu region in terms of interband transitions. Other features, like s_4 and s_6, occur however at energies in a band gap for the respective symmetry type. We demonstrate in figure 3 that these features arise from surface states.

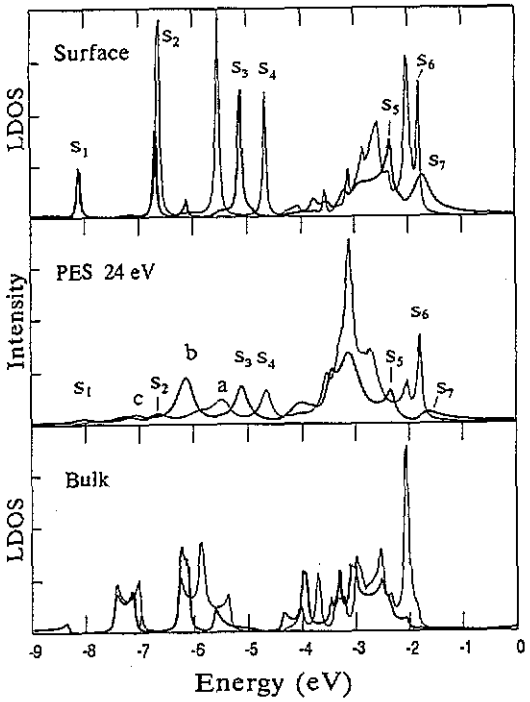

Figure 3. Surface layer density of states (top panel) and bulk LDOS (bottom panel) of Cu_3Au of symmetry types Δ_6 (thick full curves) and Δ_7 (thin full curves) for $k_\parallel = 0$ and for surface barrier located at $d_b = 0.18a$. Surface states and resonances are marked in the top panel by s_1 to s_6. The middle panel shows spin-resolved normal photoemission spectra as in figure 1.

The symmetry-resolved bulk layer densities of states in figure 3—calculated with a small constant imaginary potential value of 0.03 eV in order to emphasize features at lower energies—are seen to reflect the bulk band structure with its clear separation of the Au- and the Cu-dominated energy regions. The surface layer densities of states (top panel of figure 3) exhibit a wealth of additional features: surface states (located in a bulk band gap) like s_1, s_2, s_4 and s_6 on the one hand, and surface resonances (at band energies) like s_3, s_5 and s_7 on the other. Comparison with the photoemission spectra (central panel) shows that these surface states and resonances indeed manifest themselves in quite pronounced photoemission features.

It is instructive to project the LDOS onto Au and Cu atoms in the bulk and surface layers (figure 4). For the bulk we see, in agreement with Davenport *et al* (1988) and Sohal *et al* (1990), that the Au states are actually mainly concentrated between −5 and

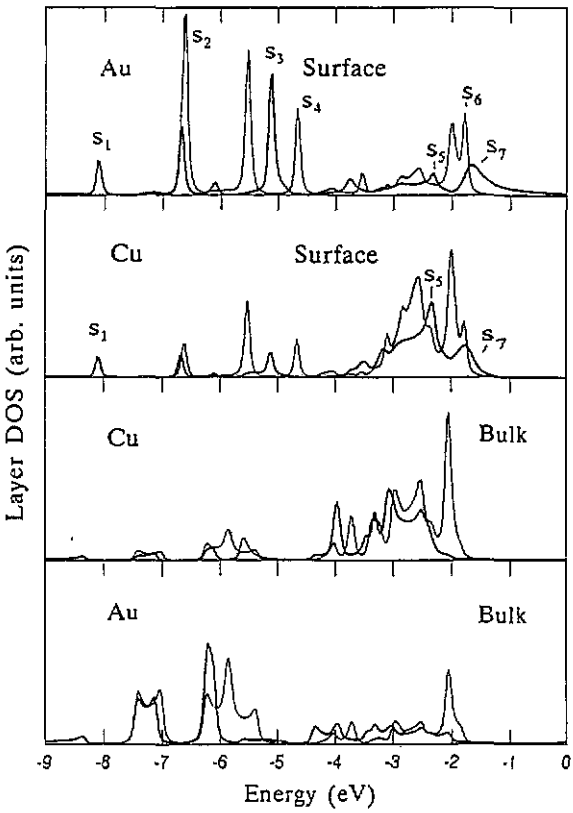

Figure 4. Projection of the surface LDOS (upper two panels) and the bulk LDOS (lower two panels) of symmetry Δ_6 (thick full curves) and Δ_7 (thin full curves) onto Au and Cu crystal atoms as indicated.

-7.5 eV, whilst Cu states dominate above -5 eV. This behaviour essentially carries over to the surface (upper two panels of figure 4). A noteworthy exception is the surface state s_6 near -1.35 eV. Although located near the upper edge of the Cu-dominated energy range, it has a larger weight on the Au spheres.

In figure 5 we show the influence of the assumed position d_b of a step-like surface potential on the calculated photoemission spectra. While the bulk interband transition peaks remain fixed in energy, the features due to surface states and resonances are seen to move towards lower energy with increasing d_b. This behaviour confirms the surface nature of these features. In particular, the Δ_7 symmetry surface-state peak s_6 is seen to lose strongly in weight while moving towards the band edge.

We now compare (in figure 6) our calculated spin-resolved spectra for $h\nu = 24$ eV with their experimental counterparts as reported by Schneider *et al* (1990). In the Au-like energy region, we find good agreement with regard to peaks a and b, which are produced by bulk interband transitions from initial states of symmetry Δ_6 and Δ_7, respectively, with wavevector component k_z near the X point. The separation of about 0.8 eV between a and b is a consequence of spin–orbit coupling. The calculated peak c occurs, as in experiment, at 7.1 eV, but is weaker. (It becomes more pronounced if we assume a smaller imaginary potential part for the occupied states). It is, however, clear that it arises from a Δ_7 initial state. The relatively high opposite-spin intensity under c is seen to stem from its broadened Δ_6-symmetry neighbour d and perhaps to some extent from the Δ_6-symmetry surface state s_2. The calculated surface states s_3 and s_4 can, with some imagination, be associated with weak experimental features at the respective energies. In the Cu-like region, the leading

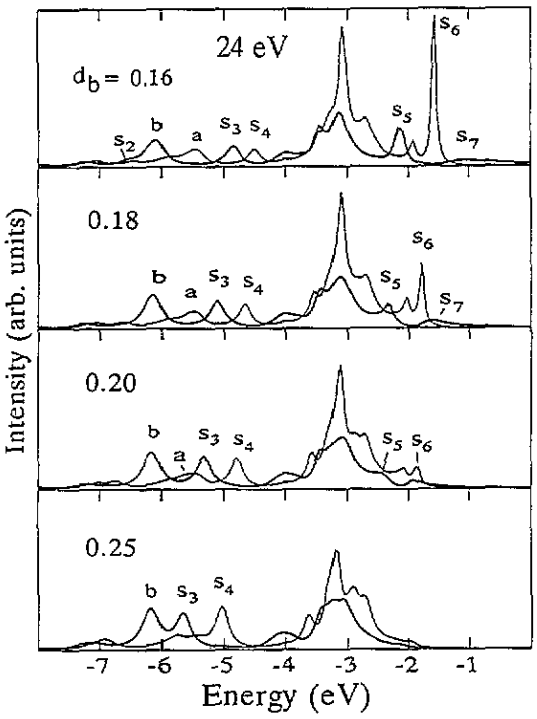

Figure 5. Spin-resolved normal photoemission spectra calculated for normally incident circularly polarized photons of energy 24 eV from Δ_6 initial states (thick full curves) and Δ_7 initial states (thin full curves) with surface barrier location d_b as indicated in the individual panels.

calculated peaks around −3.2 eV agree in existence, positions and symmetry type with experiment. The surface state s_5 shows up in experiment as a shoulder near −2.5 eV. The stronger broadening of the experimental spectra in this region may be ascribed to the relatively poor monochromator resolution (mentioned by Schneider *et al* (1990)). This also may partly explain why the sharp surface state s_6 does not show up in experiment. Figure 5 suggests that the slightly larger barrier position $d_b = 0.20$, for which s_6 is smaller and closer to the band edge, might be more appropriate. This position of the surface state is, however, at variance with detailed measurements of s_6 and its dispersion with $k_{\|}$ by Courths (1992). Calculations using the more realistic JJJ barrier form (Jones *et al* 1984) at $d_b = 0.18$ yield a substantially weaker weight of s_6, reconciling it to the experimental data of Schneider *et al* (1990) in figure 6 while retaining its energy position provided by the data of Courths (1992). Comparing the calculated spectra for upper-state real self-energy corrections by 1.0 eV and 2.5 eV (upper and central panels in figure 6), we see pronounced changes in the range between −4 and −2.5 eV. The larger correction gives better overall agreement with experiment. The spectra of the spin polarization P, which correspond via $P = (I_+ - I_-)/(I_+ + I_-)$ to the just-discussed spin-resolved intensities I_+ and I_-, are shown in the right-hand part of figure 6. The line shapes in theory and experiment are seen to be fairly similar, with the absolute values smaller by about a factor four in experiment. This reduction is to a small extent due to the fact that the degree of circular polarization of the incident light is 90% in experiment rather than 100% in theory. The main reason is presumably an inelastic background intensity present in experiment, which is almost unpolarized, i.e. composed of comparable numbers of spin-up and spin-down electrons, and is added to the actual photocurrent (as obtained by theory). In comparing experimental and theoretical spin polarization spectra, one must also bear in mind the experimental uncertainties (compare the selected error bars in figure 6), which are particularly large at

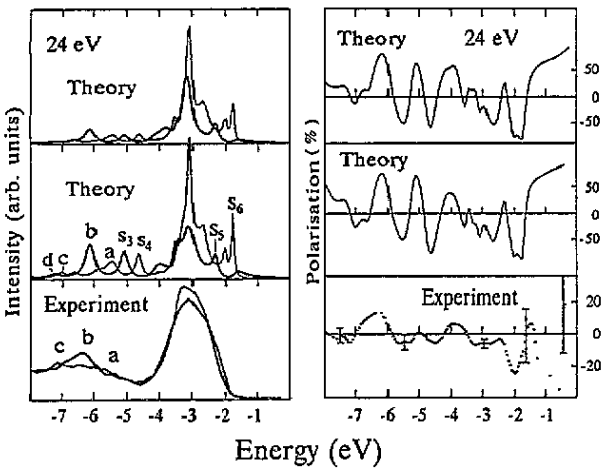

Figure 6. Spin-resolved normal photoemission intensity (left-hand column) from Δ_6 (thick full curves) and Δ_7 (thin full curves), and corresponding spin polarization (right-hand column) from $Cu_3Au(001)$ for photon energy 24 eV. The top and central panels show theoretical results for upper-state real inner-potential part 14.5 eV and 13.0 eV, respectively. Bottom panels: experimental data from Schneider *et al* 1990. The spin polarization is defined as $(I(\Delta_6) - I(\Delta_7))/(I(\Delta_6) + I(\Delta_7))$.

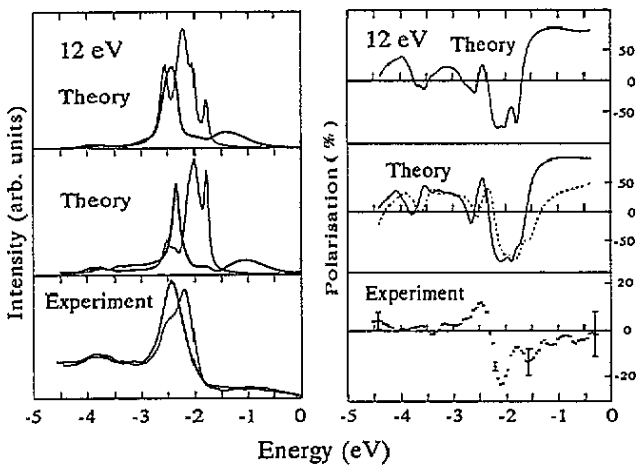

Figure 7. As figure 6, but for photon energy 12 eV. The central panel of the right-hand part contains in addition a polarization spectrum calculated for an emission angle 5° off-normal (dotted curve).

energies above about −1.5 eV as a consequence of extremely small spin-resolved intensities.

The Cu-like spectral features are better resolved in experimental data by Schneider *et al* (1990) for photon energy $h\nu = 12$ eV, which we compare in figure 7 to our calculated results. All spectra exhibit a leading peak of Δ_6 symmetry and one of Δ_7 symmetry between −2.5 and −2 eV, which can both be interpreted in terms of bulk interband transitions. The separation between them is due to the spin–orbit interaction. As is demonstrated by the top and the central panel in figure 7, their exact position and separation depend on the assumed self-energy correction for the upper states, i.e. the shift of the upper bands and consequently different k_z values probed by the transitions. The smaller self-energy correction (top panel) leads to better agreement with regard to the dominant-peak energies but the observed Δ_7 shoulder under the Δ_6 peak is better described by the larger self-energy correction (central panel). For the surface-state feature s_6, which again appears too strong in theory, we refer to the discussion given in connection with figure 6. Since the broad Δ_6 feature, which occurs in the calculated spectra near −1.4 eV (top panel) and −1 eV (central panel), depends on the upper-state self-energy correction, it has to be ascribed to a direct transition from the s-p band rather than to the surface resonance s_7 found in our layer densities of states (figure 3

and 4). This Δ_6 feature is also seen in the experimental spectra (bottom panel of figure 7), but accompanied by an even slightly larger opposite-spin feature. Since at normal emission a spin-down feature requires for its very existence (irrespective of its size) an initial state of Δ_7 symmetry, its occurrence in experiment seems rather strange, since there are no Δ_7 bulk or surface states available around -1 eV. The strong discrepancy between the calculated and measured spin polarization curves (right-hand part of figure 7) above about -1.5 eV is closely associated with this extra spin-down intensity feature. In search for an explanation we first note that the experimental uncertainty (see the error bar in the polarization data in figure 7) is a contributing but far from sufficient factor. Additional calculations for slightly off-normal electron emission (for example, the $\theta = 5°$ spin polarization spectrum shown in figure 7) revealed that in this energy range the partial intensities and consequently the spin polarization are very sensitive to small angular changes. Since experiment involves integration over a finite emission cone, strong deviations from strictly normal emission can therefore be expected. In the dominant-peak region between -2.5 and -2 eV, experimental and theoretical polarization spectra are in good agreement, while discrepancies occur again below about -2.6 eV. Bearing in mind the increase of the unpolarized inelastic background with decreasing energy, these discrepancies appear within the limits of the experimental error bars.

4. Conclusion

Applying a recently extended fully relativistic Green function theory to the semi-infinite $Cu_3Au(001)$ system in its ordered phase, we firstly obtained detailed results for the layer-, $k_\parallel$- and double group symmetry-resolved density of states. Projection onto the Au and Cu spheres shows that the electronic structure both in the bulk and at the surface separates into a Au- and a Cu-dominated energy range, but in each there is a strong admixture of the respectively other. As a consequence of such admixture of Au-character, spin–orbit induced splittings in the Cu-dominated part are larger than in pure Cu.

A wealth of new features located in the topmost atomic layer could be identified as surface states and surface resonances. Their size and energy location are very sensitive to the type and position of the assumed surface potential barrier. Refinement of the latter via comparison of calculated results with detailed high energy-resolution surface-state measurements by angle-resolved photoemission (as presently under way by Courths (1992) and co-workers) is in progress.

Our calculated spin-resolved photoemission spectra—relating individually to initial states of double group symmetry Δ_6 and Δ_7—reflect the top-layer DOS peaks. Other features, in particular four peaks in the Au-dominated energy range, can be interpreted in terms of bulk interband transitions. Comparison with the corresponding experimental spectra by Schneider *et al* (1990) shows that most observed features are reproduced by theory.

Acknowledgments

It is a pleasure for us to acknowledge lively and fruitful discussions with R Courths.

References

Ackermann B and Feder R 1985 *J. Phys. C: Solid State Phys.* **18** 1093
Courths R 1992 private communication
Courths R, Wern H, Hau U, Cord B, Bachelier V and Huefner S 1984 *J. Phys. F: Met. Phys.* **14** 1559
Davenport J W, Watson R E and Weinert M 1988 *Phys. Rev.* B **39** 9985
Eckardt H, Fritsche L and Noffke J 1984 *J. Phys. F: Met. Phys.* **14** 97
Feder R (ed) 1985 *Polarized Electrons in Surface Physics* (Singapore: World Scientific)
Ginatempo B, Guo G Y, Temmerman W M, Staunton J B and Durham P J 1990 *Phys. Rev.* B **42** 2761
Halilov S V, Tamura E, Gollisch H, Meinert D and Feder R 1993 *J. Phys.: Condens. Matter* (in press)
Hedin L and Lundqvist B I 1971 *J. Phys. C: Solid State Phys.* **4** 2064
Jennings P J, Jones R O and Weinert M 1988 *Phys. Rev.* B **37** 6113
Jepsen O, Gloetzel D and Mackintosh A R 1981 *Phys. Rev.* B **23** 2684
Jones R O, Jennings P J and Jepsen O 1984 *Phys. Rev.* B **29** 6474
Kudrnovsky J, Bose S K and Andersen O K 1991 *Phys. Rev.* B **43** 4631
Löbus S, Lau M, Courths R and Halilov S V 1993 *Surf. Sci.* (in press)
Lu Z W, Wei S H and Zunger A 1992 *Phys. Rev.* B **45** 10314
MacDonald A H, Daams J M, Vosko S H and Koelling D D 1982 *Phys. Rev.* B **25** 713
Schneider C M, Sohal G S, Schuster P and Kirschner J 1990 *Vacuum* **41** 511
Sohal G S, Carbone C, Kisker E, Krummacher S, Fattah W, Uelhoff W, Albers R C and Weinberger P 1990 *Z. Phys.* B **78** 295
Tamura E and Feder R 1989 *Solid State Commun.* **70** 205
—— 1991a *Solid State Commun.* **79** 989
—— 1991b *Europhys. Lett.* **16** 695
Tamura E, Feder R, Vogt B, Schmiedeskamp B and Heinzmann U 1989 *Z. Phys.* B **77** 129
von Barth U and Hedin L 1972 *J. Phys. C: Solid State Phys.* **5** 1629
Weinberger P, Boring A M, Albert R C and Temmerman W M 1988 *Phys. Rev.* B **38** 5357